Journal of Colloid and Interface Science **250,** 196–200 (2002)
doi:10.1006/jcis.2002.8337, available online at http://www.idealibrary.com on IDEAL®

Preparation and Structural Characterization of Activated Carbons Based on Polymeric Resin

Soo-Jin Park[1] and Woo-Young Jung

Advanced Materials Division, Korea Research Institute of Chemical Technology, P.O. Box 107, Yusong, Taejon 305-600, Korea

Received January 15, 2002; accepted March 8, 2002; published online April 29, 2002

In this work, activated carbons (ACs) with high porosity were synthesized from polystyrene-based cation-exchangeable resin (PSI) by chemical activation with KOH as the activating agent. And the influence of the KOH-to-PSI ratio on the porosity of the ACs studied was investigated by using nitrogen adsorption isotherms at 77 K and a scanning electron microscope (SEM). As a result, PSI could be successfully converted into ACs with well-developed micro- and mesopores. The specific surface area and pore volumes increased with an increase in the KOH-to-PSI ratio. However, it was found that the addition of KOH did lead to the transformation of the micropores to the meso- and macropores. From the results of pore size analysis, quite different pore size distributions were observed, resulting from the formation of new pores and the widening of the existing micropores during KOH activation. A SEM study showed that the resulting carbons possessed a well-developed pore structure and the pore size of the ACs studied increased with the KOH-to-PSI ratio. © 2002 Elsevier Science (USA)

Key Words: **activated carbon; activation; impregnation; adsorption properties; microporosity.**

INTRODUCTION

Activated carbons (ACs) are usually microporous materials that are useful in adsorption of gases or liquids and in the purificatio or recovery of chemicals (1). The usefulness of these carbons arises not only from their structural parameters, such as the specifi surface area and the pore volumes, but also from the presence of functional groups on the surface of ACs (2, 3). Although a wide range of carbonaceous materials can be converted into ACs, coal and lingocellulosic materials are the most commonly used starting materials for the production of commercial ACs. In addition, many agricultural by-products, such as nutshells, coconut shells, pecan shells, and peach stones have been found to be suitable precursors (4–7). However, society's growing concern related to the release of environmental pollutants make it necessary to prepare ACs with high surface area and pore volumes and to design new materials for their removal from gases or liquids. Recently, there have been quite a large number of studies with regard to the preparation of ACs from various polymeric materials because of high carbon yield and low ash content (8–12).

Meanwhile, the porosity of ACs is dependent not only on the kind of the starting materials employed but also on the activation methods and processes. The processes for the preparation of activated carbons can be generally divided into two categories: physical and chemical activations. Physical activation involves carbonization of the raw materials followed by gasificatio of the resulting char in the presence of some oxidizing agents (1). On the other hand, chemical activation is performed by the thermal decomposition of the precursor materials impregnated with chemical agents, such as potassium hydroxide (9), zinc chloride (13), and phosphoric acid (14). In the chemical activation, all the chemicals used act as dehydrating agents that promote the formation of cross-links, resulting in the formation of a rigid matrix that will be less susceptible to volatile loss and volume contraction upon the activation process (13). Therefore, the advantage of chemical activation is that the temperature of the process is lower since carbon burnoff is not required.

The main objectives of the present work are to prepare activated carbons from polystyrene-based ion-exchange resin (PSI) by chemical activation with potassium hydroxide and to study the effect of the KOH-to-PSI ratio on the structural properties of the fina ACs.

EXPERIMENTAL

Materials and Sample Preparation

Polystyrene-based cation-exchangeable resin (PSI, supplied from SamYang Co. of Korea) and potassium hydroxide (KOH) were used as the starting material and chemical agent, respectively. Prior to impregnation, KOH was added in a glass-stopper flas containing distilled water to obtain KOH solution having the KOH-to-PSI ratios of 0, 1, 2, and 4 by weight. Dried PSI was added to the KOH solution and then the mixture was gently stirred at 100°C for 3 h to ensure a complete reaction between KOH and PSI. After mixing, the mixture was dried at 110°C for 24 h. The KOH-loaded samples were placed in a quartz combustion boat and loaded into a horizontal cylindrical furnace (i.d. = 60 mm) in a nitrogen atmosphere, with a f ow rate of

[1] To whom correspondence should be addressed. Fax: 82 42 861 4151. E-mail: psjin@pado.krict.re.kr.

0021-9797/02 $35.00

150 ml/min. Activation was carried out by heating the samples at 10°C min^{-1}, followed by maintaining the temperature 700°C for 2 h in a furnace. After cooling, the products were crushed using a mortar and pestle to obtain particle sizes smaller than 200 μm. The crushed samples were washed sequentially with 0.5 N HCl solution at 100°C, boiling water, and f nally cold distilled water to remove residual organic and mineral matters and then dried at 110°C for 24 h. For ease of comparison, according to the KOH-to-PSI ratio the carbon products are identif ed as as-received, KPS-1, KPS-2, and KPS-4, respectively.

Adsorption Characterization

Nitrogen adsorption isotherms were measured using an ASAP 2010 (Micromeritics) at 77 K. Prior to each analysis, the samples were outgassed at 298 K for 9 h to obtain a residual pressure of less than 10^{-3} Torr. The amount of nitrogen adsorbed on ACs was used to calculate specif c surface area by means of the BET equation. Also, the BET constant (C_{BET}) obtained by the intercept of the BET equation was used for the calculation of the net of heat adsorption (ΔE):

$$C_{BET} = \exp\left[\frac{E_0 - E_L}{RT}\right] \quad [1]$$

$$\Delta E = E_0 - E_L, \quad [2]$$

where C_{BET} is a characteristic constant of the adsorbate–adsorbent, E_0 the heat of adsorption in the f rst layer, E_L the heat of liquefaction, R the gas constant, and T the Kelvin temperature. The total pore volume was estimated to be the liquid volume of nitrogen at a relative pressure of about 0.995, and the mesopore volume was obtained by subtracting the micropore volume from the total pore volume. The micropore volume was calculated using the Dubinin–Radushkevich equation (15). A liquid density of 0.808 g cm^{-3} was assumed for nitrogen in the adsorbed phase at 77 K to calculate micropore volumes (16). Also, the MP method (17) and the BJH model (18) were used to investigate micropore and mesopore size distribution, respectively.

Also, a scanning electron microscope (SEM, JEOL JSM 840A) was used to study the morphologies of the carbon surface studied.

RESULTS AND DISCUSSION

Nitrogen Adsorption Isotherms

It is well known that the chemical-to-precursor ratio is the most important parameter in the preparation of ACs using the chemical activation method (4, 9). The nitrogen adsorption isotherms on the ACs studied at different KOH-to-PSI ratios are shown in Fig. 1. It can be seen that the shape of the adsorption isotherms and the adsorption capacity signif cantly change as the KOH-to-PSI ratio increases. The adsorption isotherms of KPS-1 and KPS-2 are approximately the Type I isotherm according to BET classif cation (15), in which the knees of the

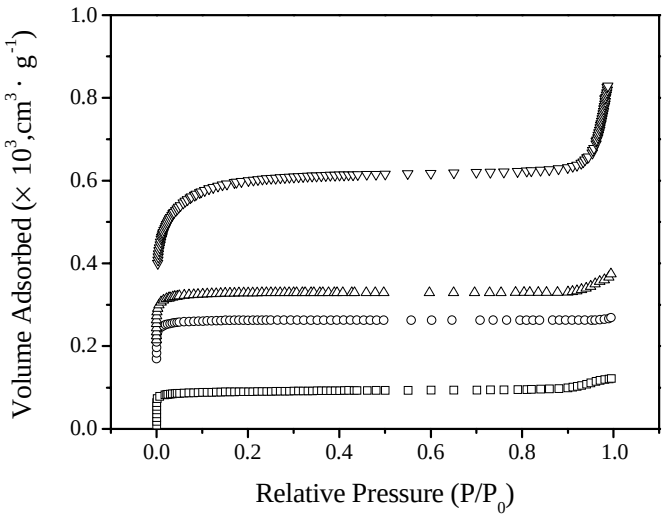

FIG. 1. Nitrogen adsorption isotherms at 77 K for the ACs studied: (□) as-received; (○) KPS-1; (△) KPS-2; (▽) KPS-4.

isotherms about $P/P_0 = 0.01$ are sharp and the plateaus are fairly horizontal. It has been known that adsorption on the microporous materials leads to an isotherm of the Type I at a lower P/P_0 (13). However, it is noted that although the shape of the adsorption isotherm for the sample KPS-2 resembles that for KPS-1, further adsorptions are observed at high relative pressure ($P/P_0 > 0.9$). This adsorption behavior indicates that the sample KPS-2 is a microporous solid having a relatively small external surface area.

Meanwhile, the nitrogen adsorption isotherm of the sample KPS-4 signif cantly differs from that of KPS-2. As shown in Fig. 1, the sample KPS-4 exhibits a more signif cant increase in adsorption at higher relative pressure, in where the knee comes to be more open and rounder and the slope of the plateau increases. And also, the nitrogen uptake signif cantly occurs at high relative pressure ($P/P_0 > 0.9$). It indicates that the meso- or macropore structure in the sample is signif cantly developed with an increase in the KOH-to-PSI ratio due to the occurrence of the widening of the existing micropores (19, 20).

The adsorption isotherms expressed in a logarithmic pressure scale are often useful for investigating the differences in the structural properties in the lower P/P_0 region ($P/P_0 \leq 0.1$) (21). Figure 2 shows the volume adsorbed of the ACs studied plotted against the logarithmic pressure. A comparison of the low-pressure segments of nitrogen adsorption isotherms for the ACs studied clearly shows that the energetic heterogeneity of KPS-4 differs from those of KPS-1 and KPS-2. However, although the low-pressure isotherm segments for the samples KPS-1 and KPS-2 are very similar, the sample KPS-2 is shifted only because of the difference in the micropore size (21).

Pore Structure Analysis

Table 1 summarizes the structural parameters at different KOH-to-PSI ratios determined from nitrogen adsorption

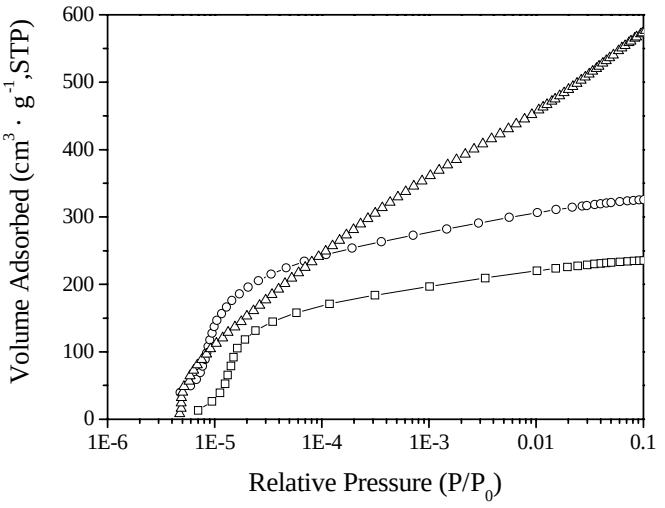

FIG. 2. Volume adsorbed of the ACs studied plotted against the logarithmic pressure: (□) KPS-2; (○) KPS-2; (△) KPS-4.

isotherms according to the BET and Dubinin–Radushkevich equations. The data show, as expected, that both BET surface area and total pore volume increase with increasing KOH-to-PSI ratio. Especially, the sample KPS-4 possesses values as high as 1947 m^2/g and 1.28 cm^3/g, which are greater than those of conventional ACs. It implies that ACs having an excellent porosity could be prepared from KOH-impregnated PSI and the increase in the KOH-to-PSI ratio results in the production of ACs with high BET surface area and total pore volume.

It is well known that the average diameter of pores is related to the net heat of adsorption (ΔE) determined from BET constant (22). The BET constant "C" values are obtained in the range of relative pressure between 0.01 and 0.05. It can be seen that the net heat of adsorption is clearly dependent on the pore diameter, not on the specif c surface area. This behavior can be due to the overlapping of the adsorption potentials from the walls of the micropores (22, 23).

Meanwhile, PSI was activated in the absence of KOH at 700°C to discuss the inf uence of KOH on the development of porosity. As shown in Fig. 1 and Table 1, the resulting sample as-received possesses a low nitrogen adsorption capacity and a specif c surface area of 357 m^2/g, suggesting that KOH plays an important role in the preparation of ACs from PSI.

Some researchers have reported that while KOH creates more micropores, the mesopore contribution is almost constant (24), and the KOH-to-PSI ratio does not have a signif cant impact on the macropore size distribution (25). Although different starting materials were used, these results contradict our study. As shown in Table 1, it can be seen that the micropore and mesopore volumes and mean pore diameter increase with an increase in the KOH-to-PSI ratio. These behaviors obviously suggest that the pore evolution can be due to the creation of new pores and widening of existing pores with increasing KOH-to-PSI ratio (13).

However, it is noted that although micro- and mesopore volumes concurrently increase with the KOH-to-PSI ratio, there is the difference in the volume fraction of the resultant ACs. The volume fraction of micropore and mesopore vs the KOH-to-PSI ratio is plotted in Fig. 3. Each volume fraction is obtained by subdividing micro- and mesopore volumes with the total pore volume. It is shown that the volume fraction of the micropore and mesopore is strongly dependent on the change in the KOH-to-PSI ratio. ACs obtained in the absence of KOH (for as-received) show the micropore volume fraction of 73% approximately. However, it varies from 98 to 65% as the KOH-to-PSI ratio increases. Mesoporosity, in turn, ranges from 2 to 35% with the KOH-to-PSI ratio.

For better characterization of the change in the microporous structure of the ACs studied, the micropore size distributions were calculated by using the MP method. The volumes of adsorbed gas were converted to liquid volumes (V_{liq}) and plotted versus the thickness of the adsorbed layer (t), which was calculated using the Harkins and Jura equation. The V–t plot was then constructed, and the micropore size distributions were extracted by drawing the slope of the linear portion of the curve (13, 26). Figure 4 shows the micropore size distributions as a function of the KOH-to-PSI ratio. It is shown that all of the pore

TABLE 1
Structural Parameters of the ACs Studied

Nomenclature	S_{BET}[a] ($m^2\ g^{-1}$)	V_t[b] ($cm^3\ g^{-1}$)	V_{micro}[c] ($cm^3\ g^{-1}$)	V_{meso}[d] ($cm^3\ g^{-1}$)	D_P[e] (Å)	ΔE[f] (kJ mol^{-1})
As-received	357	0.19	0.14	0.05	21.2	20.3
KPS-1	935	0.39	0.38	0.01	15.8	22.7
KPS-2	1337	0.58	0.50	0.08	17.3	20.6
KPS-4	1947	1.28	0.84	0.44	26.3	19.9

[a] Specif c surface area determined from the BET equation.
[b] Total pore volume.
[c] Micropore volume determined from the DR equation.
[d] Mesopore volume.
[e] Mean pore diameter.
[f] Net of heat adsorption.

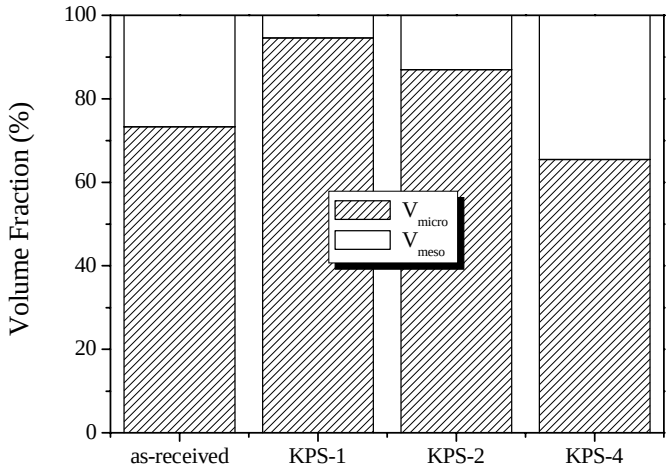

FIG. 3. Inf uence of KOH-to-PSI ratio on pore volume fraction of the ACs studied.

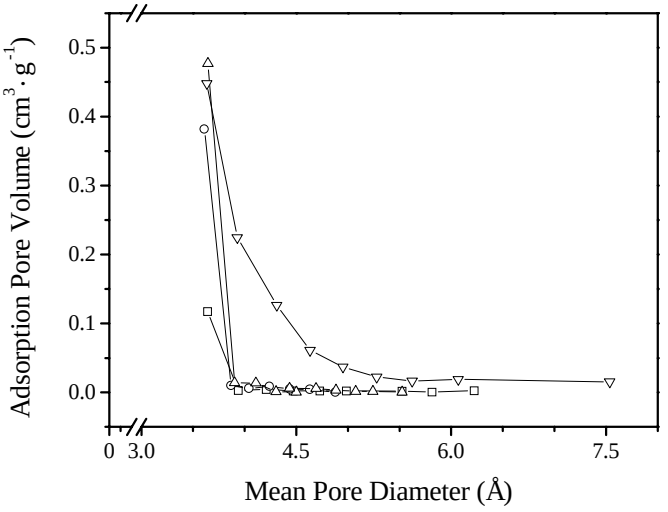

FIG. 4. Micropore size distribution determined from the MP method: (□) as-received; (○) KPS-1; (△) KPS-2; (▽) KPS-4.

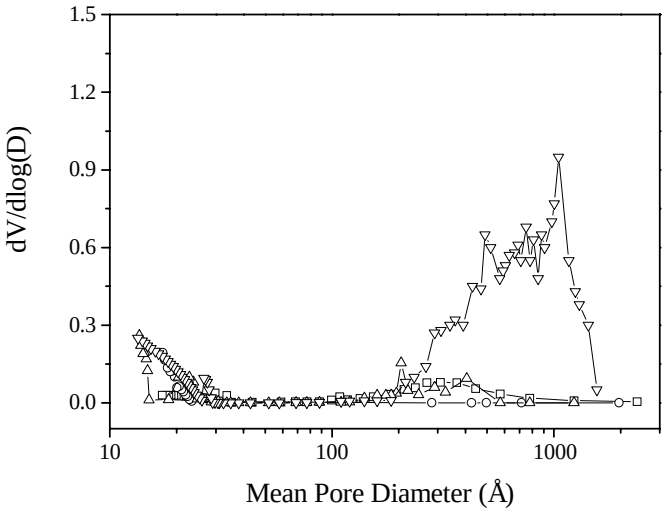

FIG. 5. Mesopore size distribution determined from the BJH model: (□) as-received; (○) KPS-1; (△) KPS-2; (▽) KPS-4.

distribution curves of the ACs studied have one peak with a maximum density at less than 4 Å, and the pore size distribution is very narrow, except for KPS-4. As mentioned above, it is found that the addition of KOH-to-PSI results in the enhancement of micropore volumes.

Figure 5 shows the mesopore size distribution evaluated by using the BJH method. It is also seen that the development of mesoporosity is strongly dependent on the change in the KOH-to-PSI ratio. As shown Fig. 5, the sample KPS-1 mainly consists of mesopores less than 30 Å in diameter. However, as the KOH-to-PSI ratio increases, the increase in mesopores is obviously observed. While the sample KPS-2 has a few mesopores less than 30 Å and in the range of 100–200 Å, KPS-4 possesses a considerable amount of mesopores below 30 Å and macropores above 500 Å.

SEM Observation

The porous structure of the ACs studied was observed by using a scanning electron microscope (SEM). Figure 6 shows the SEM photographs of the ACs studied. As shown in Fig. 6, the resulting carbons do have a well-developed pore structure and the shape of the external surface signif cantly changes in the increase in the KOH-to-PSI ratio. It is largely attributed to

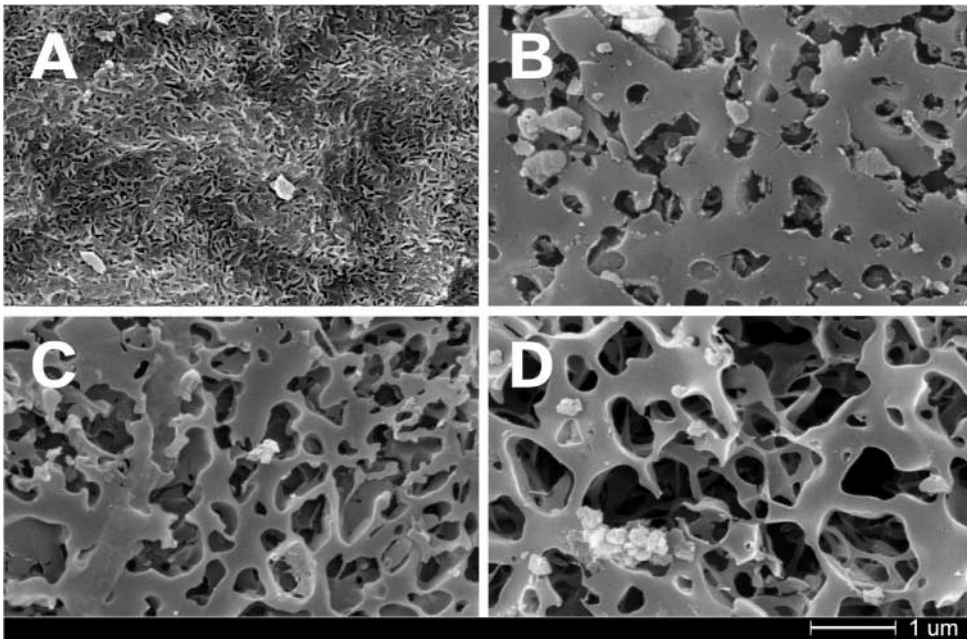

FIG. 6. SEM photographs of the ACs studied: (A) as-received; (B) KPS-1; (C) KPS-2; (D) KPS-4 (×20000).

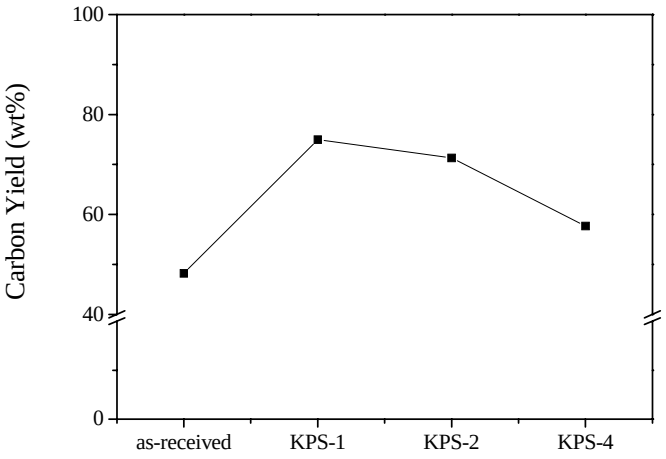

FIG. 7. Effect of the KOH-to-PSI ratio on the carbon yield.

carbon gasif cation by the reduction of K_2CO_3 and K_2O formed below 500°C as shown in Eqs. [3] and [4] (27).

$$K_2CO_3 + 2C \rightarrow 2K + 3CO \quad [3]$$

$$K_2O + C \rightarrow 2K + CO. \quad [4]$$

Also, at high KOH-to-PSI ratio a signif cant amount of gaseous products, such as water and CO_2, are produced due to excessive KOH molecules as shown in Eq. [5] and these gases are responsible for some additional gasif cation of carbon, resulting in the creation of new pores and the widening of the existing pores during KOH activation (4).

$$2KOH \rightarrow K_2O + H_2O \quad [5a]$$

$$H_2O + C \rightarrow CO + H_2 \quad [5b]$$

To investigate the effect of the KOH-to-PSI ratio on the carbon yield, the yield of the ACs studied was calculated by using the following equation (6),

$$\text{Carbon yield (in wt\%)} = [W_1/W_2] \times 100, \quad [6]$$

where W_1 and W_2 are the weights of the activated carbon product and the KOH-loaded PSI, respectively.

Figure 7 shows the relationship between the KOH-to-PSI ratio and the carbon yield. It is shown that the carbon yield decreases as the KOH-to-PSI ratio increases. This behavior can result from the opening up of closed pores and widening of the existing pores.

CONCLUSION

In this work, it was conf rmed that PSI could be successfully converted to ACs with high porosity. The surface area and pore volume of the ACs studied increased with an increase in the KOH-to-PSI ratio. However, the ACs studied possessed markedly different pore size distribution with KOH-to-PSI ratio. It could be seen from the SEM photographs that the increase in the porosity of the resulting carbons was due to the occurrence of gasif cation on the external surface during activation. It was then concluded that KOH played an important role in the development of pores and was a promising activating agent for the preparation of ACs derived from PSI.

ACKNOWLEDGMENT

This work was supported by Grant 2000-2-30100-011-3 from the Basic Research Program of the Korea Science & Engineering Foundation.

REFERENCES

1. Cheremisinoff, P. M., and Ellerbusch, C., "Carbon Adsorption Handbook." Ann Arbor Science, Ann Arbor, MI, 1978.
2. Park, S. J., and Park, B. J., and Ryu, S. K., *Carbon* **37,** 1223 (1999).
3. Park, S. J., and Kim, K. D., *J. Colloid Interface Sci.* **212,** 186 (1999).
4. Ahmadpour, A., and Do, D. D., *Carbon* **35,** 1723 (1997).
5. Hu, Z., and Srinivasan, M. P., *Microporous Mesoporous Mater.* **27,** 11 (1999).
6. Ahmedna, M., Marshall, W. E., and Rao, R. M., *Bioresource Technol.* **71,** 103 (2000).
7. Molina-Sabio, M., Rodriguez-Reinoso, F., Caturla, F., and Selles, M. J., *Carbon* **34,** 457 (1996).
8. Park, S. J., and Kim, K. D., *Carbon* **39,** 1741 (2001).
9. Teng, H., and Wang, S. C., *Carbon* **38,** 817 (2000).
10. Petrov, N., Budinova, T., Razvigorova, M., Ekinci, E., Yardim, F., and Minkova, V., *Carbon* **38,** 2069 (2000).
11. Marzec, M., Tryba, B., Kalenczuk, R. J., and Morawski, A. W., *Polym. Adv. Technol.* **10,** 588 (1999).
12. Nakagawa, H., Watanabe, K., Harada, Y., and Miura, K., *Carbon* **37,** 1455 (1999).
13. Khalili, M. R., Campbell, M., Sandi, G., and Golas, J., *Carbon* **38,** 1905 (2000).
14. Guo, J., and Lua, A. C., *Microporous Mesoporous Mater.* **32,** 111 (1999).
15. Gregg, S. J., and Sing, K. S. W., "Adsorption, surface area and porosity." Academic Press, New York, 1982.
16. Dubinin, M. M., and Stoeckli, H. F., *J. Colloid Interface Sci.* **75,** 34 (1980).
17. Mikhail, R. S., Brunauer, S., and Bodor, E. E., *J. Colloid Interface Sci.* **26,** 45 (1968).
18. Lippens, B. C., and de Boer, J. H., *J. Catal.* **4,** 319 (1965).
19. Warhurst, A. M., Fowler, G. D., McConnachie, G. L., and Pollard, S. J. T., *Carbon* **35,** 1039 (1997).
20. Park, S. J., and Jung, W. Y., *Carbon*, in press.
21. Choma, J., and Jaroniec, M., *Langmuir* **13,** 1026 (1997).
22. Dubinin, M. M., *Carbon* **27,** 457 (1989).
23. Nguyen, C., and Do, D. D., *Langmuir* **15,** 3608 (1999).
24. Ahmadpour, A., and Do, D. D., *Carbon* **34,** 471 (1996).
25. Gonzalez-Serano, E., Cordero, T., Rodriguez-Mirasol, J., and Rodriguez, J. J., *Ind. Eng. Chem. Resources* **12,** 1723 (1997).
26. Lowell, S., and Shields, J. E., "Powder Surface Area and Porosity." Chapman & Hall, New York, 1991.
27. Hayashi, J., Kazehaya, A., Muroyama, K., and Watkinson, A. P., *Carbon* **38,** 1873 (2000).